0026-895X/01/6003-480–487$3.00
MOLECULAR PHARMACOLOGY
Vol. 60, No. 3
950/928172
Mol Pharmacol 60:480–487, 2001
Printed in U.S.A.

Glycosylation of the Human Prostacyclin Receptor: Role in Ligand Binding and Signal Transduction

ZHIBING ZHANG, SANDRA C. AUSTIN, and EMER M. SMYTH

Center for Experimental Therapeutics, University of Pennsylvania, Philadelphia, Pennsylvania

Received March 13, 2001; accepted June 8, 2001

This paper is available online at http://molpharm.aspetjournals.org

ABSTRACT

Prostacyclin, a potent vasodilator and inhibitor of platelet aggregation, acts through a cell-surface G protein-coupled receptor [prostacyclin (IP)]. The human (h) IP contains two consensus sites for *N*-linked glycosylation (N^7 and N^{78}). However, the role of glycosylation is unknown. Mutant receptors (N^7-Q^7,N^{78}-Q^{78} and N^7,N^{78}-Q^7,Q^{78}) were generated by replacing N^7 and/or N^{78} with Q's. Receptor glycosylation was similar in the wild-type and N^7-Q^7 and was inhibited with tunicamycin. N^{78}-Q^{78} and N^7,N^{78}-Q^7,Q^{78} demonstrated little or no glycosylation. Membrane localization was reduced for each mutant concomitant with impaired glycosylation. Partial localization to the plasma membrane allowed direct examination of the effect of glycosylation on IP function. High-affinity binding to N^7-Q^7 was similar (K_d = 21.7 ± 1.7 nM, n = 4) to that of the wild-type receptor (K_d = 24.3 ± 3.6 nM, n = 4), despite a reduced value for B_{max} (0.35 ± 0.03 fmol/mg of protein versus 3.34 ± 0.52 fmol/mg of protein, n = 4). Binding to N^{78}-Q^{78} (B_{max} = 0.27 ± 0.03 fmol/mg of protein, n = 3; K_d = 149.1 ± 11.1, n = 3) and N^7,N^{78}-Q^7,Q^{78} (no specific binding) was further impaired. Agonist-induced adenylyl cyclase activation was reduced in N^7-Q^7 cells, whereas N^{78}-Q^{78} cells responded only to high concentrations of iloprost and N^7,N^{78}-Q^7,Q^{78} were unresponsive. Inositol phosphate generation was evident only with the wild-type. Only the wild-type and N^7-Q^7 receptors underwent agonist-induced sequestration. Our findings demonstrate greater glycosylation at N^{78} compared with N^7. The extent of *N*-linked glycosylation of hIP may be important for membrane localization, ligand binding, and signal transduction.

Prostacyclin (PGI_2), the major product of arachidonic acid in vascular endothelium (Habib et al., 1997), transduces its potent antiplatelet, vasodilator, and antiproliferative actions via a G protein-coupled receptor (GPCR), the prostacyclin receptor (IP). Human IP (hIP) is coupled to stimulation of both adenylyl cyclase and phospholipase C (PLC) (Boie et al., 1994; Namba et al., 1994; Smyth et al., 1996). Agonist-induced phosphorylation and desensitization of hIP is mediated primarily by protein kinase C-dependent receptor phosphorylation (Smyth et al., 1996, 1998), whereas activation-dependent receptor sequestration may be phosphorylation independent and proceed via at least two distinct pathways (Smyth et al., 2000)

Most GPCRs contain one or two potential *N*-linked glycosylation sites (Asp-X-Ser/Thr, where X represents any amino acid except a proline (Gavel and Heijne, 1990), located at the N terminus and/or extracellular loops (Marshall et al., 1972; Bause et al., 1983). The carbohydrate moieties of glycoproteins are generally are believed to be important for intracellular trafficking, stability, secretion, and/or protein folding, enzymatic activity, and additional structural functions (Frost et al., 1991; Rodriguez et al., 1995; Ray et al., 1998; Walsh et al., 1998; Zhou and Tai, 1999; Boer et al., 2000; Kataoka et al., 2000). All eicosanoid receptors that have been cloned so far (prostaglandin D_2, prostaglandin $F_{2\alpha}$, PGI_2, two thromboxane A_2 (TP) and four prostaglandin E2 (EP) (Coleman et al., 1994), have *N*-glycosylation sites. This modification seems to play important functional roles in the GPCR superfamily although the impact varies from receptor to receptor. Glycosylation of TP and EP3α are necessary both for correct sorting to the plasma membrane and for normal ligand binding (Huang and Tai, 1998; Walsh et al., 1998). In contrast, whereas plasma membrane localization of glycosylation-deficient β-adrenergic receptors (Rands, 1990) or EP3β receptors (Boer et al., 2000) was reduced, ligand binding and signal transduction were preserved.

Two potential *N*-glycosylation sites (N^7 and N^{78}) are located in the hIP's N terminus and first extracellular loop, respectively. We previously demonstrated that hIP is expressed as a glycoprotein in HEK 293 cells (Smyth et al., 1996); however, the functional importance of this receptor modification has not been examined. In this study, we sought to determine the functional importance of *N*-glycosylation of

This work was supported by National Institute of Health Grants HL62250 and HL57847 and American Heart Association Grant 9906209U (to E.M.S).

ABBREVIATIONS: PGI_2, prostacyclin; GPCR, G protein-coupled receptor; hIP, human prostacyclin receptor; PLC, phospholipase C; TP, thromboxane A_2 receptor; EP, prostaglandin E_2 receptor; HEK, human embryonic kidney; GFP, green fluorescent protein; ELISA, enzyme-linked immunosorbent assay; HA, hemagglutinin; PBS, phosphate-buffered saline; FI, fluorescent intensity.

hIP. We used site-directed mutagenesis of the N^7 and N^{78} residues of the hIP to explore the significance of *N*-glycosylation for hIP function. Our results indicated that *N*-glycosylation of hIP, especially at N^{78}, is important for membrane expression, ligand binding, and signal transduction.

Materials and Methods

(*R*)-Phycoerythrin and Cy3-conjugated AffiniPure F(ab′)2 fragment goat anti-mouse IgG (H+L) were from Jackson ImmunoResearch (West Grove, PA). Anti-human golgin-97 was from Molecular Probes (Eugene, OR). PEGFP-N3 was obtained from CLONTECH Laboratories, Inc (Palo Alto, CA). Poly-lysine and tunicamycin were purchased from Sigma (St. Louis, MO). All cell culture reagents, G418, Albumax were from Invitrogen (Carlsbad, CA). *N*-[1-(2,3-Dioleoyloxy)propyl]-*N*,*N*,*N*-trimethylammonium methylsulfate, FuGENE transfection reagent, complete protease inhibitor tablets, and 4-nitrophenyl phosphate were obtained from Roche Biochemicals (Indianapolis, IN). AG 1-X8 resin (formate form) was purchased from Bio-Rad (Hercules, CA). Dr. Kathleen Metters (Merck Frosst, Quebec, Canada) generously donated the hIP cDNA. PNGase F was from New England BioLabs Inc (Beverly, MA). Oligonucleotides were from Cybersyn (Philadelphia, PA).

Generation of Green Fluorescent Protein-hIP Fusion Protein and Site-Directed Mutagenesis. The green fluorescent protein (GFP) was fused to the C-terminal end of the hemagglutinin (HA) tagged hIP (HAhIP) to generate the construct HAhIP-GFP as described previously (Smyth et al., 1996; Smyth et al., 2000). Primers were designed to mutate N^7 to Q^7 (sense, 5′ GCG GAT TCG TGC AGG CAG CTC ACC TAC GTG CGG) and N^{78} to Q^{78} (sense: 5′ GTG GCC TAT GCG CGC CAG AGC TCC CTG CTG GGC), in HAhIP-GFP. Mutagenesis was performed using the MORPHTM site-specific plasmid DNA Mutagenesis kit (Eppendorf-5 Prime, Inc., Boulder, CO). The mutated receptors were termed N^7-Q^7,N^{78}-Q^{78} and N^7,N^{78}-Q^7,Q^{78}. Mutagenesis was confirmed by DNA sequencing.

Cell Culture and Transfection. COS-7 and HEK 293 cells (American Type Culture Collection; Manassas, VA) were maintained in Dulbecco's modified Eagle's medium supplemented with 10% heat-inactivated fetal bovine serum, 50 U/ml penicillin, 50 μg/ml streptomycin, 25 mM HEPES, and 2 mM glutamine. COS-7 cells were transfected transiently with FuGENE transfection reagent in six-well cell culture plates. For stable transfections, HEK cells were seeded at 1.5×10^6 cells/100-mm dish and, the next day, transfected with 10 μg/dish DNA by liposome-mediated transfer (*N*-[1-(2,3-dioleoyloxy)propyl]-*N*,*N*,*N*-trimethylammonium methylsulfate), as described previously (Smyth et al., 1996, 1998).

Western Blotting. Cells were lysed (radioimmuniprecipitation assay: 50 mM Tris/5 mM EDTA, pH 8.0, containing 150 mM NaCl, 1% Nonidet P40, 0.1% SDS, 0.5% deoxycholic acid, 1 tablet/50 ml complete protease inhibitor cocktail), drawn through a 23-gauge needle six times and centrifuged at 14,000 rpm. Proteins were resolved on 8% SDS polyacrylamide gels and transferred to nitrocellulose. Receptors were visualized by treating immunoblots, first blocked with 5% nonfat milk in Tris-buffed saline/Tween 20 (50 mM Tris/250 mM NaCl, pH 7.6 containing 1% Tween 20), for 2 h at room temperature, followed by incubation with anti-HA (1:1500 dilution) and then incubation with a horseradish peroxidase-conjugated anti mouse IgG (1:5000 dilution). Antigen-antibody complexes were visualized with the use of enhanced chemiluminescence.

Deglycosylation of IP. Removal of asparagine-linked mannose, hybrid and complex oligosaccharides with PNGaseF was carried out according to the manufacturer's instructions. Membrane proteins (30 μg) were denatured in 0.5% SDS, 1% β-mercaptoethanol at 100°C for 10 min. Deglycosylation was carried out for 60 min at 37°C in 50 mM sodium phosphate buffer, pH 7.5, containing 1% Nonidet P-40, and reactions were stopped by the addition of SDS-polyacrylamide gel sample buffer.

Immunofluoresence Microscopy. Cells were seeded into lysine coated two chamber slides (Nalge Nunc International Corp, Naperville, IL). One to two days later, cells were fixed and permeabilized in 100% methanol at −80°C for 7 min. The Golgi apparatus was stained with anti-human golgin-97 (1 μg/ml, 60 min) followed by Cy3-conjugated anti-mouse (1:1000 dilution, 60 min). GFP and Cy3 fluorescence was examined by confocal microscopy within 1 week.

Radioligand Binding. Membrane proteins were prepared from confluent 100-mm dishes as follows. Cells were washed once with phosphate-buffered saline and scraped into 20 mM Tris, pH 7.4, containing 4 mM EDTA, and complete protease inhibitor. Cells were lysed and drawn although a 23-gauge needle 10 times, and membrane fractions were collected by centrifugation at 115,000*g* for 1 h at 4°C. The resulting pellet was resuspended in the same buffer and stored at −80°C for further use. Radioligand binding studies were carried out using membrane proteins (50 μg/reaction) in 10 mM HEPES, pH 7.4, contain 10 mM MnCl as described previously (Smyth et al., 1996). Nonspecific binding was measured in the presence of a 500-fold excess of unlabeled iloprost. Saturation binding data were analyzed using Prism 2.0 (Graphpad Software, San Diego, CA) to calculate K_d and B_{max} values for binding.

Flow Cytometry. Cells were detached from tissue culture plates with 1 mM EDTA in PBS and washed with PBS containing 1% BSA and 0.1% NaN_3. The detached cells were resuspended in PBS and 1% BSA containing anti-HA monoclonal antibody (or a control isotype IgG1κ) for 60 min, followed by (*R*)-phycoerythrin-conjugated AffiniPure F(ab′)2 fragment goat anti-mouse IgG) for 30 min at 4°C. Cells were analyzed for fluorescence intensity by flow cytometry, after one further wash. Dead cells were detected by low forward- and right-angle scatter and excluded from the analysis.

Internalization of HahIP. Cells were seeded on 0.1 mg/ml lysine-coated, glass-bottomed plates (MatTek Corp., Ashland, MA), for confocal microscopy, or 24-well dishes for ELISA and, 24 to 48 h later, treated with iloprost (1 μM). Real time internalization of receptors was examined by confocal microscopy of GFP. Cell surface localization of HAhIP-GFP was quantified by ELISA after fixation of the cells (4% paraformaldehyde in PBS, 4°C, 10–15 min), as described previously (Smyth et al., 2000).

Measurement of cAMP. Cells, grown to confluence in 12-well plates coated with 0.1 mg/ml lysine, were treated with iloprost (10 min at 37°C). Reaction were terminated by aspiration and cAMP was extracted with ice-cold 65% ethanol for 30 min. Samples were dried under vacuum and reconstituted in assay buffer, and cAMP was quantified by radioimmunoassay, as described previously (Smyth et al., 1996, 1998). Dose-response data were analyzed using the CalcuSyn dose-effect analysis program (Biosoft, Milltown, NJ) to calculate EC_{50} values.

Inositol Phosphate Production. Cells, grown to 70 to 80% confluence in 12-well plates coated with 0.1 mg/ml lysine, were labeled overnight with 2 μCi/ml [myo-^{3}H]inositol in DMEM (without inositol) containing 0.5% Albumax. Thirty minutes before stimulation, cells were treated with 20 mM LiCl at 37°C. After stimulation for 10 min at 37°C, the reactions were terminated by aspiration. Total inositol phosphates were extracted, recovered, and quantified as described previously (Smyth et al., 1996, 1998).

Statistical Analysis. Data were compared by Student's *t* test or analysis of variance for multiple comparisons. *P* value of <0.05 was considered significant.

Results

Expression and Characterization of *N*-Glycosylation HAhIP-GFP and Mutant Receptors in COS-7 Cells and HEK Cells. We have previously shown that HAhIP is glycosylated in stably transfected HEK 293 cells (Smyth et al., 1996) and that the addition of the HA (Smyth et al., 1996) and the GFP tags (Smyth et al., 2000) does not effect receptor

signaling or localization. In the current study, COS-7 cells were transiently transfected with HAhIP-GFP and the receptor was examined by Western blotting. Wild-type hIP resolved as three bands (Fig. 1A). Only the lowest band (68 kDa, which represents the deglycosylated receptor plus the 27-kDa GFP) remained after treatment of cells with tunicamycin (2 μg/ml), an inhibitor of glycosylation, indicating that, similar to the HAhIP in HEK 293 cells, HAhIP-GFP was glycosylated in COS-7 cells. Thus, hIP glycosylation is not confined to a particular cell line.

Immunoblot analysis revealed that N^7-Q^7 had characteristics similar to those of the wild-type HAhIP-GFP, except that the uppermost band was absent (Fig. 1A, lanes 1 and 3). This upper band was lost when glycosylation at N^7 was prevented, and thus it seems to represent the fully glycosylated receptor. Some glycosylation, presumably at N^{78}, remains. Both the N^{78}-Q^{78} and N^7,N^{78}-Q^7,N^{78} receptors resolved as a single band with a molecular mass of 68 kDa (Fig. 1A, lanes 4 and 5), similar to the tunicamycin-treated cells (Fig. 1A Lane 2), representing the fully deglycosylated receptor.

HEK 293 cells stably expressing the three mutant receptors were established to investigate further the role of *N*-linked glycosylation. Several cell lines were screened for receptor expression. HAhIP-GFP (Fig. 1B, lane 1) resolved as a single band with a molecular mass of 68 kDa and a broad band of 68 to 100kDa, representing the deglycosylated and glycosylated receptors (plus GFP), respectively, as reported previously (Smyth et al., 2000). The N^7-Q^7 mutant demonstrated similar characteristics, although a shift in the relative amounts of glycosylated to nonglycosylated receptor, compared with wild-type, was evident (Fig. 1B, lane 2). This mutant, therefore, was at least partially glycosylated in HEK 293 cells, similar to COS-7 cells. N^{78}-Q^{78} receptors (Fig. 1B, lane 3) demonstrated extensive deglycosylation, whereas the N^7,N^{78}-Q^7,Q^{78} mutant (Fig. 1B, lane 4) showed no receptor glycosylation. The ratio of glycosylated to nonglycosylated receptor, calculated by densitometric analysis of representative Western blots, followed the sequence HAhIP-GFP > N^7-Q^7 $\gg$ N^{78}-Q^{78} > N^7,N^{78}-Q^7,Q^{78} demonstrating that, although both N^7 and N^{78} are glycosylated, the majority of glycosylation occurred at the latter residue. All receptors resolved as a single deglycosylated band when membrane proteins were deglycosylated with PNGase F (Fig. 1C). Cell lines 1, 2d, 3i, and 4m (Fig. 1B) were used for remaining experiments.

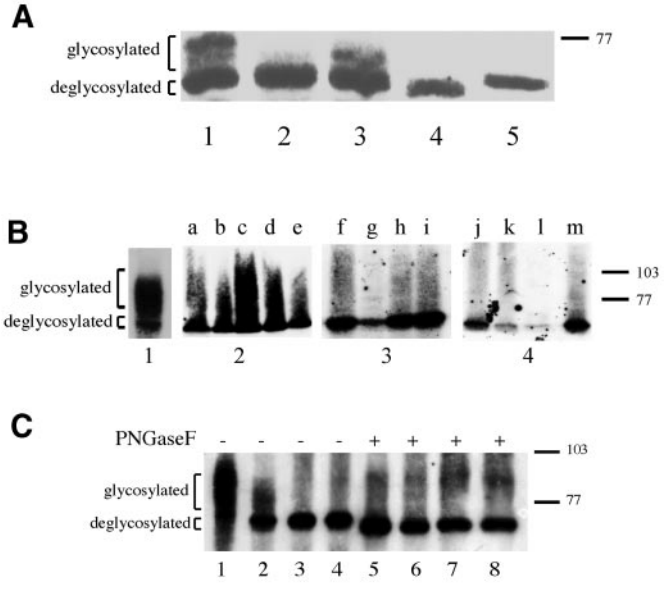

Fig. 1. Expression of HAhIP-GFP and mutant receptors in COS-7 and HEK cells. Cells were lysed and 30 μg total protein was loaded onto 8% polyacrylamide gels, transferred to polyvinylidene difluoride membranes and immunoblotted with anti-HA antibody. Molecular masses are in reported in kiloDaltons. A, transient expression of HAhIP-GFP in COS-7 cells. Lane 1, wild-type HAhIP-GFP; lane 2: wild-type HAhIP-GFP + tunicamycin (2 μg/ml); lane 3: N^7-Q^7; lane 4: N^{78}-Q^{78}; lane 5: N^7, N^{78}-Q^7,Q^{78}. B, screening of the HEK 293 cell lines stably transfected with mutant HAhIP-GFPs. 1, wild-type HAhIP-GFP cell; 2, a–e, N^7-Q^7 clones; 3, f–i, N^{78}-Q^{78} clones; 4, j–m, N^7,N^{78}-Q^7,Q^{78} clones. C, analysis of PNGase F digested mutant HAhIP-GFPs. Lanes 1–4, HAhIP-GFP, N^7-Q^7, N^{78}-Q^{78}, N^7, N^{78}-Q^7, Q^{78}; lanes 5–8: HAhIP-GFP, N^7-Q^7, N^{78}-Q^{78}, N^7, N^{78}-Q^7, Q^{78} digested with PNGase F.

Role of *N*-Linked Carbohydrates in IP Cell Surface Expression. Analysis of GFP localization by confocal microscopy demonstrated that, similar to the wild-type HAhIP-GFP, each of the three mutant receptors were localized to the plasma membrane (Fig. 2A). However, the relative intensity of membrane localization appeared to be reduced in each of the mutated cell lines, compared with the wild-type. In addition, dense cytoplasmic localization of receptor, which colocalized with a marker for the Golgi apparatus, was evident in each mutant cell lines (Fig. 2B) demonstrating retention of the glycosylation deficient mutants in the Golgi. Colocalization, which was minimal in wild-type cells (Fig. 2B, a) was evident when glycosylation at N^7 was absent (Fig. 2B, b) and more extensive when N^{78} was mutated (Fig. 2B, c and d).

Cell surface expression of hIP was quantified by flow cytometric analysis of HA expression, as shown in Fig. 3. Because of the extracellular location of the HA tag, the value of florescent intensity was taken as a measurement of the relative amount of the cell membrane receptor expression. Fluorescent intensity was corrected for background fluorescence using an IgG1κ, the same isotype as anti-HA. The relative expression of HAhIP-GFP in the membrane was reduced in each of the three mutant cell lines (Fig. 3), in agreement with the confocal microscopy data. Interestingly, reduced membrane expression, together with retention in the Golgi, seemed to correlate with the extent of glycosylation; N^{78}-Q^{78} and N^7,N^{78}-Q^7,Q^{78} showed less membrane localization (Fig. 3), and a more extensive colocalization with anti-glogin 97 (Fig. 2B, c and d), compared with N^7-Q^7 (Figs. 2B, b and 3) However, despite the progressive loss of glycosylation and cell surface localization, a substantial level of the mutant receptors appeared to localize normally (Fig. 3), allowing us to address directly the role of glycosylation in receptor function.

Role of IP Glycosylation in Ligand Binding. Ligand binding to HAhIP-GFP mutant receptors was examined in saturation binding experiments using membranes prepared from each of the four cell lines. Specific [^{3}H]iloprost binding was evident in all cases except the double mutant (Fig. 4, Table 1), although radioligand binding was reduced in both N^7-Q^7 and N^{78}-Q^{78} compared with the wild-type receptor. The extent of receptor glycosylation seemed to produce differential effects on radioligand binding. Thus, although HAhIP-GFP and N^7-Q^7 had similar K_d values for [^{3}H]iloprost binding, the latter showed a much lower B_{max} (Table 1). In contrast, N^{78}-Q^{78} cells had a low B_{max} value, similar to that of N^7-Q^7 cells, but the ligand affinity was greatly reduced

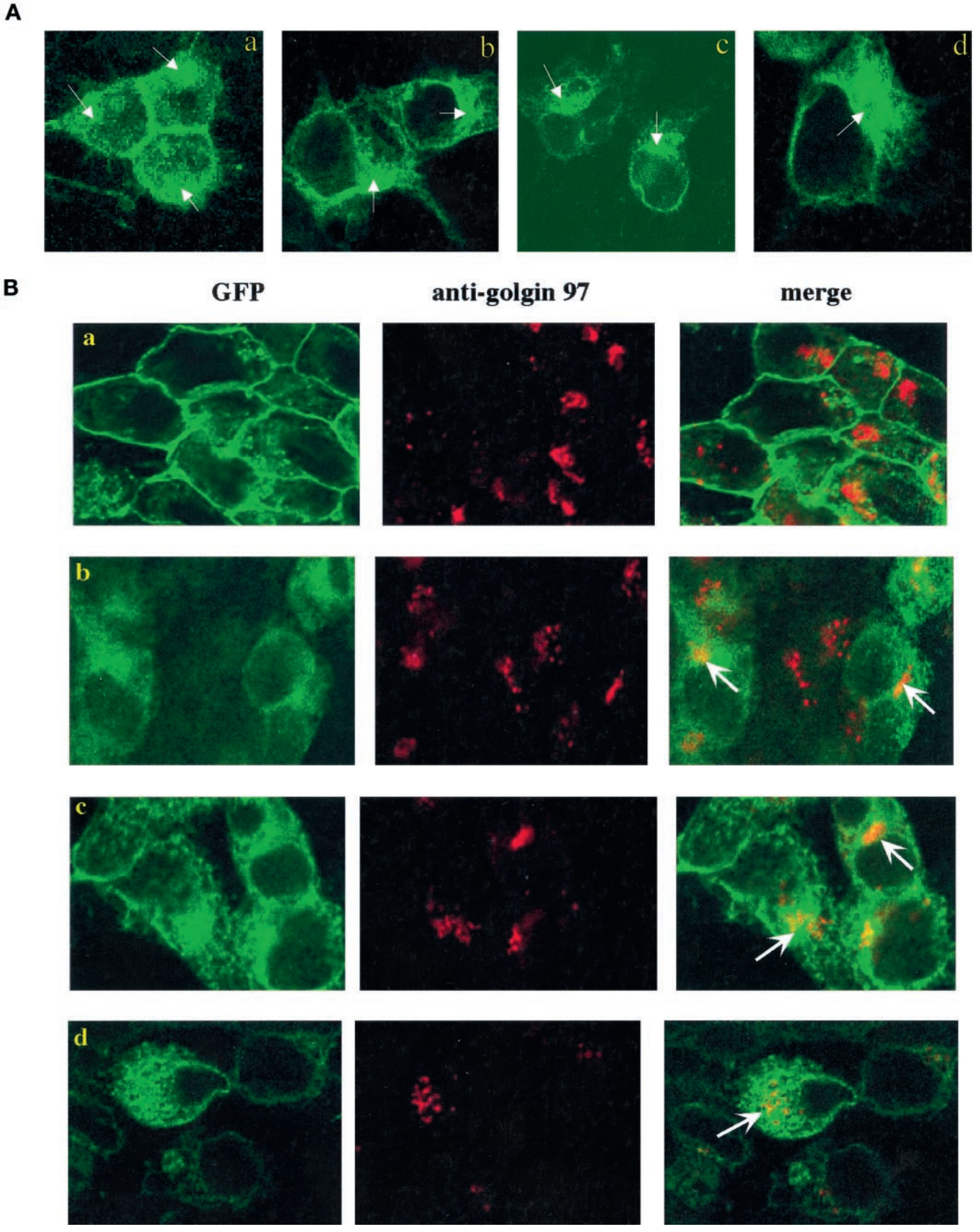

Fig. 2. Confocal microscopy HEK 293 cells expressing mutant HAhIP-GFPs. a, wild-type HAhIP-GFP cells; b, N^{7}-Q^{7} cells; c, N^{78}-Q^{78} cells; d, N^{7}, N^{78}-Q^{7}, Q^{78} cells. A, arrows indicate dense cytoplasmic localization of the GFP-tagged receptors. B, cells were treated with anti-golgin 97 to stain the Golgi apparatus. Colocalization of GFP-tagged receptors (green) with the Golgi (red) can been seen (yellow) when the data was merged. Arrows highlight areas of colocalization

compared with both the wild-type HAhIP-GFP and N^7-Q^7 cells. Finally, binding was not detected in N^7,N^{78}-Q^7,Q^{78} cells.

Analysis of Intracellular Signaling. Human IP couples to activation of both adenylyl cyclase and phospholipase C in HEK 293 cells and these features are unaffected by the addition of the HA and/or GFP tags (Smyth et al., 1996, 2000). Intracellular signaling of HAhIP-GFP was dramatically altered by mutation of the *N*-glycosylation sites. Generation of cAMP was reduced in the N^7-Q^7 cell line. Iloprost induced a concentration-dependent increase in cAMP generation in HAhIP-GFP cells (EC_{50} = 0.51 ± 0.1 nM, n = 3), which reached a maximum level of 150.4 ± 15 pmol cAMP/10^6 cells at 5 nM iloprost (Fig. 5). In contrast, cAMP production at 5 nM iloprost was reduced to 75 ± 20 pmol cAMP/10^6 cells (n = 3) in N^7-Q^7 cells and the concentration-response curve was shifted to the right, demonstrating an increase in EC_{50}. A low level of cAMP was generated through N^{78}-Q^{78} at very high concentrations of iloprost only while N^7,N^{78}-Q^7,Q^{78} did not transduce this signal (Fig. 5). Thus, similar to membrane localization and radioligand binding, iloprost-induced activation of adenylyl cyclase was reduced relative to the extent of receptor glycosylation. In contrast, iloprost-induced generation of inositol phosphate was absent in each of the three mutant cell lines regardless of their glycosylation state (Fig. 6).

Role of *N*-Linked Carbohydrates in IP Internalization. Recently, we reported that the hIP is internalized in response to agonist stimulation (Smyth et al., 2000). Iloprost induced sequestration of HAhIP-GFP was evident only in the wild-type and N^7-Q^7 cell line and not in N^{78}-Q^{78} or N^7,N^{78}-Q^7,Q^{78} (Fig. 7), suggesting a role for glycosylation in receptor trafficking. Similar results were obtained by confocal microscopy (data not shown).

Discussion

Many GPCRs, including the hIP (Smyth et al., 1996), have been shown to undergo *N*-linked glycosylation. However, the role played by this post-translational modification in GPCR biology is not clear. The hIP contains two asparagine residues, N^7 and N^{78}, that are potential *N*-linked glycosylation sites. We examined the role of this modification in hIP cellular localization and function.

We have previously demonstrated that hIP, stably expressed in HEK 293 cells, is a glycoprotein and can be converted to the deglycosylated form with PNGase F (Smyth et al., 1996). In the current study, glycosylated forms of HAhIP-GFP were evident in both transiently transfected COS-7 cells and stably transfected HEK 293 cells, demonstrating that glycosylation of hIP is not cell specific. We generated three mutant HAhIP-GFP receptors in which N^7 or N^{78} was replaced with Q, alone or in combination. These mutant recep-

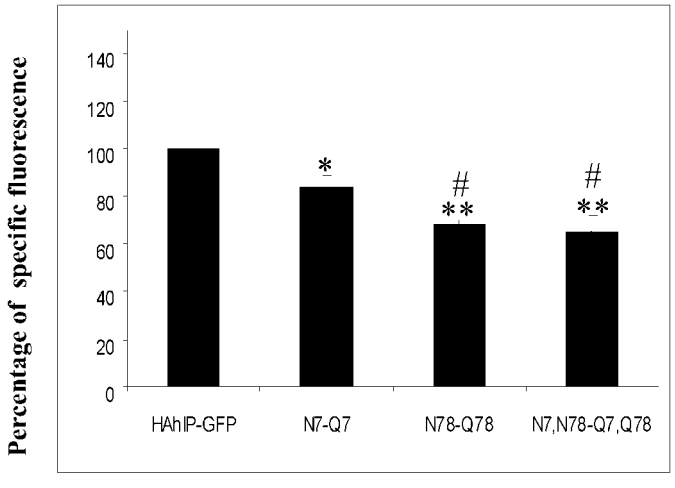

Fig. 3. Flow cytometric analysis of cell-surface expression of mutant HAhIP-GFPs. Cell surface HA expression was examined in each of the four cell lines, by flow cytometry, using the anti-HA monoclonal antibody or a control isotype. Specific fluorescent intensity (FI) of each cell line was corrected for the control FI. The percentage of specific FI relative to the wild-type HAhIP-GFP (100%) was calculated in each cell line. Data are the mean ± SEM of three independent experiments. *$P < 0.05$; **$P < 0.01$ compared with wild-type HAhIP-GFP. #$P < 0.05$ compared with N^7-Q^7 cells.

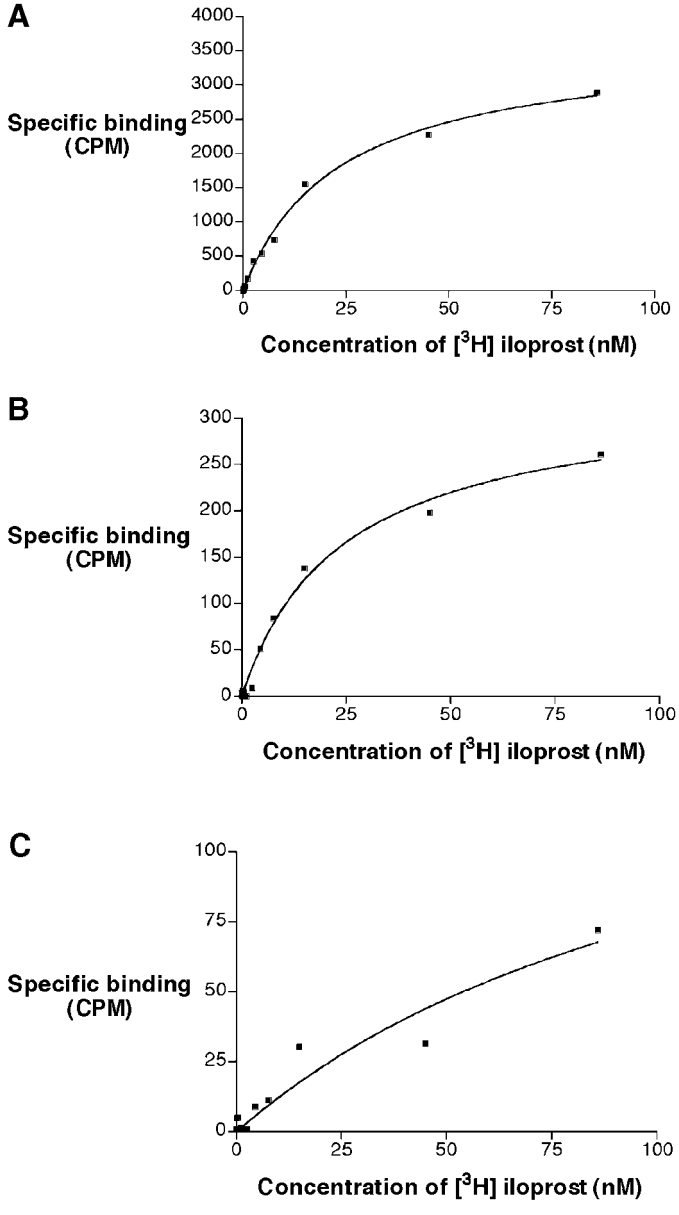

Fig. 4. Saturation binding of ^{3}H-iloprost to membranes prepared from HAhIP-GFP mutant cell lines. Membrane proteins (50 μg) were incubated at 30°C for 30 min with [^{3}H]iloprost. Nonspecific binding was quantified in the presence of 5 μM unlabeled iloprost. Data are from a representative experiment that was repeated with similar results. a, wild-type HAhIP-GFP cells; b, N^7-Q^7 cells; c, N^{78}-Q^{78} cells.

tors were transiently expressed in COS-7 cells, stably expressed in HEK 293 cells and examined by Western blotting. Both glycosylation sites were used, because mutation of either asparagine residue led to reduced receptor glycosylation. However, the loss of glycosylation was more extensive in N^{78} mutants, demonstrating the greater importance of this site for hIP glycosylation. Receptor glycosylation followed the sequence HAhIP-GFP > N^7-Q^7 ≫ N^{78}-Q^{78} > N^7,N^{78}-Q^7,Q^{78}. Interestingly, glycosylation at N^7 was not apparent in the N^{78}-Q^{78} mutant, expressed in COS-7 cells (Fig. 1A, lane 3), suggesting some interaction between the two sites.

N-linked glycosylation has been demonstrated to play a role in subcellular distribution of many membrane-associated proteins (Nagai et al., 1997; Ray et al., 1998; Zhou and Tai, 1999). The cellular trafficking of a glycoprotein often depends on its correct glycosylation; carbohydrate moieties are thought to act as tags for the correct sorting of proteins to their subcellular target (Scheiffele et al., 1995; Gut et al., 1998; Benting et al., 1999). Non/partially glycosylated or improperly folded proteins are, in contrast, retained in the endoplasmic reticulum (Hammond and Helenius, 1995). Studies have demonstrated that the loss of the carbohydrate moieties associated with membrane receptors led to reduced membrane expression (Ray et al., 1998; Walsh et al., 1998; Boer et al., 2000; Kataoka et al., 2000). In agreement with these reports, cell surface expression of HAhIP-GFP was reduced in all three mutant cell lines (Fig. 3). Indeed, direct examination of mutant receptors, by confocal microscopy, indicated that each was retained in the cytoplasm, which colocalized with a Golgi marker, although membrane localization was still evident. Impaired membrane localization, together with increased retention in the Golgi, followed a similar sequence to glycosylation, namely HAhIP-GFP > N^7-Q^7 > N^{78}-Q^{78} ≥ N^7,N^{78}-Q^7,Q^{78}. Thus, it seems that glycosylation of hIP plays a role in its correct translocation through the Golgi apparatus to the plasma membrane. However, membrane localization of each mutant receptor was evident, despite the progressive loss of glycosylation, suggesting that pathway does not exclusively determine the subcellular localization of HAhIP.

A direct functional role for GPCR glycosylation has been demonstrated (Frost et al., 1991; Huang et al., 1995; Rodriguez et al., 1995; Pang et al., 1999; Elleman et al., 2000; Kataoka et al., 2000; Nagai et al., 2000; Nagayama et al., 2000; Zhou et al., 2000). The partial membrane localization of HAhIP-GFP mutant receptors, despite major differences in glycosylation, allowed us to examine directly the role played by glycosylation in hIP ligand binding and signal transduction. It is generally thought that the seventh transmembrane domain, highly conserved among the prostanoid receptor family (Ushikubi et al., 1995) forms a critical portion of the ligand binding pocket for GPCR (Baldwin et al., 1995). However, reports have demonstrated that *N*-linked glycosylation of TP and the EP3 isoform of the PGE_2 receptor are necessary for optimal ligand binding (Huang et al., 1995; Huang and Tai, 1998; Walsh et al., 1998), although this was not the case for EP3β (Boer et al., 2000). As with surface localization, binding of iloprost to HAhIP-GFP was reduced in all three glycosylation deficient mutant receptors, albeit to varying extents (Table 1). However, the loss of cell surface receptor localization (20–40%, Fig. 3) could not account for the dramatic decrease in B_{max} for each mutant receptor (>90%, Table 1). Thus, the deficiency in glycosylation seems to affect directly ligand binding. Whereas the B_{max} value was reduced in cells expressing the N^7-Q^7 mutant, the K_d value remained unchanged, indicating that this receptor was capable of binding iloprost with high affinity. In contrast, a reduced B_{max}, together with an increased K_d, in N^{78}-Q^{78} expressing cells, and loss of specific binding in N^7,N^{78}-Q^7,Q^{78} cells, suggests a direct relationship between the extent of glycosylation and the receptors ability to ligate its agonist. Although it may be argued that the mutant cell lines simply expressed less receptor protein, compared with the wild-type controls, this is not likely to adequately explain the changes in ligand binding. Each receptor was transfected under the same conditions using the same CMV promoter and cell lines were selected for further work on the basis of equivalent expression by Western blotting and confocal microscopy (Figs. 1B and 2). It is more likely that the progressive reduction in ligand binding was coincident with reduced glycosylation. This is particularly evident when N^7-Q^7 was compared with N^{78}-Q^{78}; both cell lines have the same B_{max} value for iloprost binding, demonstrating equivalent receptor expression levels, but the loss of glycosylation at N^{78} dramatically reduced binding affinity. These data suggest that glycosylation is required for optimal binding of ligand to hIP and that N^{78} may play a more significant role in determining the efficiency with which the receptor binds its ligand.

We have previously shown that hIP can couple to both activation of adenylyl cyclase, through Gs, and increased generation of inositol phosphates, probably via Gq-PLC activation (Smyth et al., 1996). Not surprisingly, signaling through the glycosylation-deficient HAhIP-GFPs was reduced compared with the fully glycosylated control (Figs. 5 and 6). Coupling to cAMP generation followed the same pattern as glycosylation; N^7-Q^7 was more efficient compared with either N^{78} mutant, the double mutant being the weakest of the three. It may be that the shift in the cAMP dose-response curve observed in the N^7-Q^7 mutant cells was simply a result of the 10-fold reduction in B_{max} (Table 1) and not as a result of changes in glycosylation per se. Although we cannot discount this possibility, the marked difference in cAMP production in N^{78}-Q^{78} cells compared with N^7-Q^7 cells, despite their equivalent B_{max} (Fig. 5, Table 1), demonstrates a direct role of glycosylation at N^{78} in signal transduction and implies a similar explanation for the impaired coupling

TABLE 1

Binding characteristics of HAhIP-GFP mutant receptors

Saturation binding of [^{3}H]iloprost was carried out using membranes prepared from each cell line. Data are the mean ± SEM from three to four experiments.

	HAhIP-GFP (n = 4)	N^7-Q^7 (n = 4)	N^{78}-Q^{78} (n = 3)	N^7,N^{78}-Q^7,Q^{78}
B_{max} (fmol/mg of protein)	3.34 ± 0.52	0.35 ± 0.03*	0.27 ± 0.03*	N.D.
K_d (nM)	24.3 ± 3.6	21.7 ± 1.7	149.1 ± 11.1*	N.D.

* $p < 0.05$ compared with HAhIP-GFP.
N.D., not detectable.

of N^7-Q^7 to Gs. In contrast to cAMP production, activation of PLC is absent in all three cell lines, regardless of glycosylation efficiency, even when iloprost was used at concentrations of up to 10 μM. Thus, normal glycosylation of hIP is required for optimum Gs-coupling and, similar to ligand binding, glycosylation at N^{78} seems to be more significant for signal transduction through this pathway. The absolute dependence of the Gq-PLC pathway on receptor glycosylation indicates that glycosylation may direct hIP coupling to multiple G proteins, raising the intriguing possibility that the cell may control the formation of different receptor-G protein pairs via changes in receptor glycosylation.

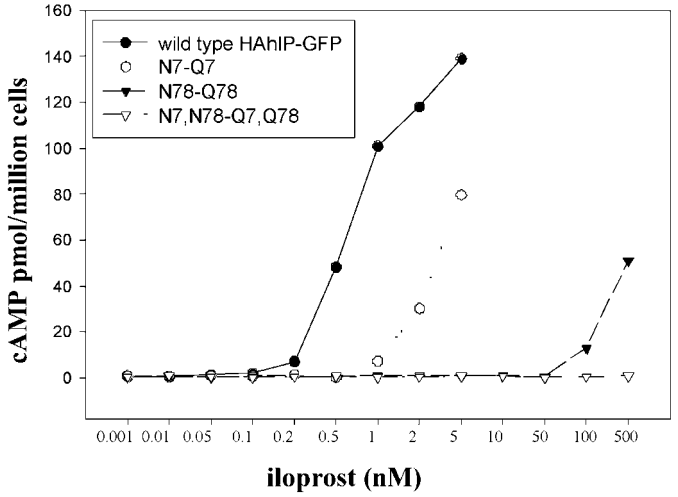

Fig. 5. Intracellular cAMP production in HEK 293 cells expressing mutant HAhIP-GFP. Cells were stimulated with increasing concentration of iloprost for 10 min at 37°C. Intracellular cAMP was extracted and quantified as outlined under *Materials and Methods*. The results were calculated as the fold increase over basal levels (cAMP production in the absence of agonist stimulation). Data are from one experiment that was repeated three to five times with similar results.

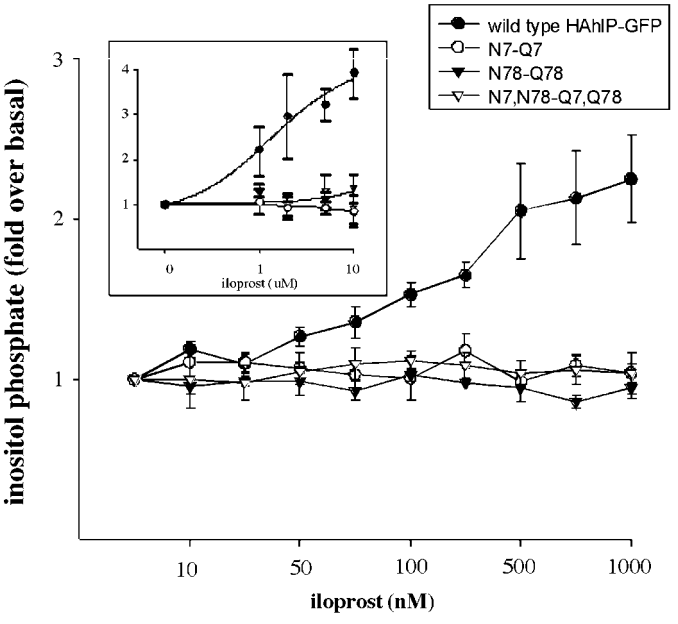

Fig. 6. Total inositol phosphate production in HEK 293 cells expressing mutant HAhIP-GFP. Cells were treated with increasing concentrations of iloprost for 10 min at 37°C, and inositol phosphates extracted and quantified as outlined under *Materials and Methods*. The results were calculated as the fold increase over basal levels (inositol phosphate production in the absence of agonist stimulation). The inset shows inositol phosphate generation resulting from stimulation with 1 to 10 μM iloprost. Data are mean ± SEM from three to four independent experiments, each performed in duplicate.

Agonist-induced sequestration of HAhIP from the cell membrane into the intracellular space proceeds in a phosphorylation-independent manner that seems to involve both dynamin-dependent and -independent pathways and is mediated through the C-terminal region of the receptor (Smyth et al., 2000). We examined receptor sequestration in each of the three glycosylation deficient HAhIP-GFPs. Iloprost stimulated receptor internalization in both the HAhIP-GFP and N^7-Q^7 cells, but not in N^{78}-Q^{78} or N^7,N^{78}-Q^7,Q^{78} cells. It may be argued the N^{78} mutants do not internalize simply because of impaired ligand binding. However, both N^7-Q^7 and N^{78}-Q^{78} cells display similar B_{max} values for iloprost binding, although the K_d value is reduced in the latter case (Table 1). Given the high dose of iloprost (1 μM) used in the sequestration experiments, both receptors would be expected to substantially bind ligand. However, sequestration is evident only in the case of N^7-Q^7, suggesting that glycosylation plays a direct role in hIP trafficking from the plasma membrane to the cytoplasm. The mechanism by which the absence of carbohydrate moieties at the N terminus can affect sequestration, mediated through the C terminus, is unclear and currently under investigation. Certainly, it seems that sequestration occurs independently of coupling to PLC; N^7-Q^7 did not couple to increased generation of inositol phosphates, but was sequestered in a manner similar to the that of wild-type receptor. Note that despite the ability of N^{78}-Q^{78} to mediate some activation of cAMP production, treatment of N^{78}-Q^{78} cells with a high concentration of iloprost did not elicit a sequestration response (Figs. 5 and 7). Sequestration of hIP may, therefore, be at least partially independent of signal transduction and require glycosylation at N^{78}.

In summary, our findings demonstrate that both potential *N*-linked glycosylation sites are used in the hIP N^{78} to a greater extent. *N*-linked glycosylation of hIP, particularly at N^{78}, seems to play roles in membrane localization, ligand binding, signal transduction, and receptor sequestration. The mechanism through which glycosylation of hIP affects its function is not known. Recently, a new family of proteins known as receptor activity modifying proteins was described.

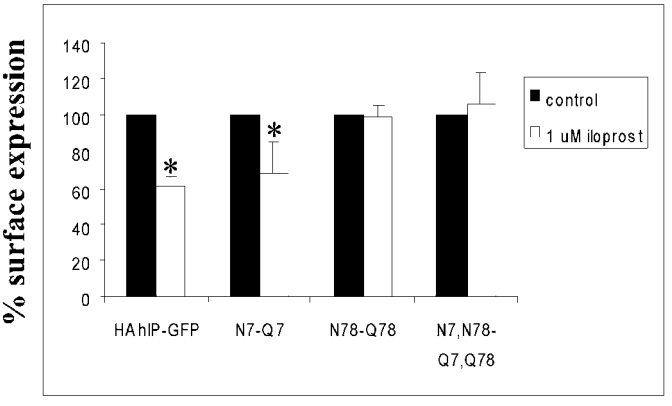

Fig. 7. Internalization of cell surface wild-type and deglycosylated hIP. Cells were treated with 1 μM iloprost for 60 min. Surface HA expression was measured by ELISA and calculated as the percentage of absorbance in the absence of iloprost. Data are expressed as mean ± SEM from five independent experiments, each performed in triplicate. *$P < 0.01$ with reference to control.

These proteins physically interact with GPCRs (Leuthauser et al., 2000) and alter their glycosylation state, ligand binding, and signal transduction properties (Fraser et al., 1999). Although it is not known whether receptor activity modifying proteins exist for hIP, the interaction of such an accessory protein may depend on glycosylation. How glycosylation at the N terminus can affect events throughout the receptor, including at distal regions such as the C terminus, is not clear but suggests a further level of complexity through which the cell can control and alter its responses to GPCR activation.

Acknowledgments

We thank Ekaterina Kostetskaia for technical assistance.

References

Baldwin JM (1995) Structure and function of receptor coupled to G proteins. *Curr Opin Cell Biol* **6:**180–190.

Bause E (1983) Structural requirements of *N*-glycosylation of proteins. Studies with proline peptides as conformational probes. *Biochem J* **209:**331–336.

Benting JH, Rietveld AG and Simons K (1999) *N*-Glycans mediate the apical sorting of a GPI-anchored, raft-associated protein in Madin-Darby canine kidney cells. *J Cell Biol* **146:**313–320.

Böer U, Rube F, Möller U and Püschel GP (2000) Requirement of *N*-glycosylation of the prostaglandin E2 receptor EP3β for correct sorting to the plasma membrane but not for correct folding. *Biochem J* **350:**839–847.

Boie Y, Rushmore TH, Darmon-Goodwin A, Grygorczyk R, Slipetz DM, Metters KM and Abramovitz M (1994) Cloning and expression of a cDNA for the human prostanoid IP receptor. *J Biol Chem* **269:**12173–12178.

Coleman RA, Smith WL and Narumiya S (1994) International union of pharmacology classification of prostanoid receptors: properties, distribution and structure of the receptors and their subtypes. *Pharmacol Rev* **46:**205–229.

Elleman TC, Frenkel MJ, Hoyne PA, McKern NM, Cosgrove L, Hewish DR, Jachno KM, Bentley JD, Sankovich SE and Ward CW (2000) Mutational analysis of the *N*-linked glycosylation sites of the human insulin receptor. *Biochem J* **347:**771–779.

Fraser NJ, Wise A, Brown J, McLatchie LM, Main MJ and Foord SM (1999) The amino terminus of receptor activity modifying protein is a critical determinant of glycosylation state and ligand binding of calcitonin receptor-like receptor. *Mol Pharmacol* **55:**1054–1059.

Frost GH, Bergmann JS and Carney DH (1991) Glycosylation of high-affinity thrombin receptors appears necessary for thrombin binding. *Biochem Biophy Res Commun* **180:**349–355.

Gavel Y and Heijne GV (1990) Sequence differences between glycosylated and non-glycosylated Asn-X-Thr/Ser acceptor sites: implications for protein engineering. *Protein Eng* **3:**433–442

Gut A, Kappelar F, Hyka N, Balda MS, Hauri HP and Matter K (1998) Carbohydrate-mediated Golgi to cell surface transport and apical targeting of membrane proteins. *EMBO J* **17:**1919–1929.

Habib A, Vezza R, Creminon C, Maclouf J and FitzGerald GA (1997) Rapid, agonist-dependent phosphorylation in vivo of human thromboxane receptor isoforms. Minimal involvement of protein kinase C. *J Biol Chem* **272:**7191–7200

Hammond C and Helenius A (1995) Quality control in the secretary pathway. *Curr Opin Cell Biol* **7:**523–529.

Huang C and Tai HH (1995) Ser-268 and *N*-linked glycosylation play an important role in ligand binding of EP3 subtype of the prostaglandin (PG)E2 receptor. *FASEB J* **9:**116.

Huang C and Tai HH (1998) Prostaglandin E2 receptor EP3alpha subtype: the role of *N*-glycosylation in ligand binding as revealed by site-directed mutagenesis. *Prostaglandins Leukot Essent Fatty Acids* **59:**265–271

Kataoka H, Kume N, Miyamoto S, Minami M, Murase T, Sawamura T, Masaki T, Hashimoto N and Kita T (2000) Biosynthesis and post-translational processing of lectin-like oxidized low density lipoprotein receptor-1 (LOX-1). *N*-linked glycosylation affects cell-surface expression and ligand binding. *J Biol Chem* **275:**6573–6579.

Leuthauser K, Gujer R, Aldecoa A, McKinney RA, Muff R, Fischer JA and Born W (2000) Receptor-activity-modifying protein 1 forms heterodimers with two G-protein-coupled receptors to define ligand recognition. *Biochem J* **351:**347–351

Marshall RD (1972) Glycoproteins. *Annu Rev Biochem* **41:**673–702.

Nagai K, Ihara Y, Wada Y and Taniguchi N (1997) *N*-Glycosylation is requisite for the enzyme activity and Golgi retention of *N*-acetylglucosaminyltransferase III. *Glycobiology* **7:**769–776.

Nagai R, Matsumoto K, Ling X, Suzuki H, Araki T and Horiuchi S (2000) Glycolaldehyde, a reactive intermediate for advanced glycation end products, plays an important role in the generation of an active ligand for the macrophage scavenger receptor. *Diabetes* **49:**1714–1723.

Nagayama Y, Nishihara E, Namba H, Yamashita S and Niwa M (2000) Identification of the sites of asparagine-linked glycosylation on the human thyrotropin receptor and studies on their role in receptor function and expression. *J Pharmacol Exp Ther* **295:**404–409.

Namba T, Oida H, Sugimoto Y, Kakizuka A, Negishi M, Ichikawa A and Narumiya S (1994) cDNA cloning of a mouse prostacyclin receptor. Multiple signaling pathways and expression in thymic medulla. *J Biol Chem* **269:**9986–9992.

Pang RT, Ng SS, Cheng CH, Holtman MH, Miller LJ and Chow BK (1999) Role of *N*-linked glycosylation on the function and expression of the human secretin receptor. *Endocrinology* **140:**5102–5111

Rands E, Candelore MR, Cheung AH, Hill WS, Strader CD and Dixon RA (1990) Mutational analysis of beta-adrenergic receptor glycosylation. *J Biol Chem* **265:**10759–10764.

Ray K, Clapp P, Goldsmith PK and Spiegel AM (1998) Identification of the sites of *N*-linked glycosylation on the human calcium receptor and assessment of their role in cell surface expression and signal transduction. *J Biol Chem* **273:**34558–34567.

Rodriguez CG, Cundell DR, Tuomanen E, Kolakowski LF, Gerard C and Gerard NP (1995) The role of *N*-glycosylation for functional expression of the human platelet-activating factor receptor. *J Biol Chem* **270:**25178–25184.

Scheiffele P, Peranen J and Simons K (1995) *N*-Glycans as apical sorting signals in epithelial cells. *Nature (Lond)* **378:**96–98.

Smyth EM, Austin SC, Reilly MP and FitzGerald GA (2000) Internalization and sequestration of the human prostacyclin receptor. *J Biol Chem* **275:**32037–32045.

Smyth EM, Li WH and FitzGerald GA (1998) Phosphorylation of the prostacyclin receptor during homologous desensitization. *J Biol Chem* **273:**23258–23266.

Smyth EM, Nestor PV and FitzGerald GA (1996) Agonist-dependent phosphorylation of an epitope-tagged human prostacyclin receptor. *J Biol Chem* **271:**33698–33704

Ushikubi F, Hirata M and Narumiya S (1995) Molecular biology of prostanoid receptors: an overview. *J Lipid Mediat Cell Signal* **12:**343–359.

Walsh MT, Foley JF and Kinsella BT (1998) Characterization of the role of *N*-linked glycosylation on the cell signaling and expression of the human thromboxane A_2 receptor α and β isoforms. *J Pharmacol Exp Ther* **286:**1026–1036.

Zhou AT, Assil I and Abou-Samra AB (2000) Role of asparagine-linked oligosaccharides in the function of the rat PTH/PTHrP receptor. *Biochemistry* **39:**6514–6520

Zhou H and Tai HH (1999) Characterization of recombinant human CXCR4 in insert cells: Role of extracellular Domain and *N*-glycosylation in ligand binding. *Arch Biochem Biophys* **369:**267–276.

Address correspondence to: Dr. Emer M Smyth, Center for Experimental Therapeutics, University of Pennsylvania, 816 BRB2/3, 421 Curie Blvd., Philadelphia, PA 19104-6160. E-mail: emer@spirit.gcrc.upenn.edu